DOI: 10.1002/ejic.201100467

ESR Study of Light-Induced Valence Tautomerism of a Dinuclear Co Complex

Yoshio Teki,*[a] Mugen Shirokoshi,[a] Shinji Kanegawa,[b] and Osamu Sato*[b]

Keywords: Light-induced valence tautomerism / ESR / Cobalt / Charge transfer / Glasses

Light-induced valence tautomerism (LIVT) of a dinuclear complex, $[\{Co(dpqa)\}_2(dhbq)](PF_6)_3$ (**1**), was investigated by ESR analysis of $dhbq^{3-}$. LIVT phenomena were observed in the sample diluted in the glass matrix as well as that in powder form. The signal decay and the relaxation were analyzed by double exponential fitting; the results suggest a two-step mechanism. Quantum mechanical tunneling was clearly observed in the glass matrix.

Introduction

Valence tautomeric complexes undergoing metal–ligand electron transfer have been attracting increasing interest.[1–5] Light-induced valence tautomerism (LIVT) and light-induced excited spin state trapping (LIESST) are the most promising properties for molecular memory devices.[6–11] In our previous work,[12] LIVT of $[\{Co(dpqa)\}_2(dhbq)](PF_6)_3$ (**1**) [dhbq = deprotonated 2,5-dihydroxy-1,4-benzoquinone, dpqa = bis(2-pyridylmethyl)-*N*-(quinolin-2-methyl)amine], shown in Figure 1, was investigated mainly by magnetic susceptibility measurements. The low-temperature and high-temperature phases of **1** are Co^{III}-$dhbq^{3-}$-Co^{III}, with the $dhbq^{3-}$ radical (S = 1/2) and a low-spin (LS) Co^{III} state ($Co^{III,LS}$; S = 0), and Co^{III}-$dhbq^{2-}$-Co^{II}, with a high-spin (HS) Co^{II} state (S = 3/2), respectively. The phase transition is driven by entropy. The spin state of the dhbq bridging ligand changes from S = 1/2 ($dhbq^{3-}$) to S = 0 ($dhbq^{2-}$) [12,13] and that of the Co metal site changes from S = 0 (Co^{III}) to S = 3/2 (Co^{II}). Thus, we can monitor the phase transition by the change in the spin state of the ligand.[12–14] In this work, the LIVT and relaxation processes of **1** were investigated by monitoring the ESR signals of the $dhbq^{3-}$ radical both in the powder sample and in the glass matrix. Previously, LIVT was also studied in the sample diluted in polymer, and the importance of quantum mechanical tunneling (QT) in valence tautomeric materials was pointed out by pulsed laser photolysis.[15] Very recently, it has been suggested by studies of LIVT in solid solution that the bistability is related to the single-molecule properties rather than to the cooperative effect of the lattice.[16] In this work, in addition to the powder sample, we observed LIVT phenomena in the sample diluted in a glass matrix, in which no cooperative effect is expected. This finding has clearly shown that the bistability is related to the single-molecule properties. The signal decay and the relaxation were analyzed by double exponential fitting, which indicated the possibility of a two-step mechanism. QT phenomena were clearly observed in the glass matrix.

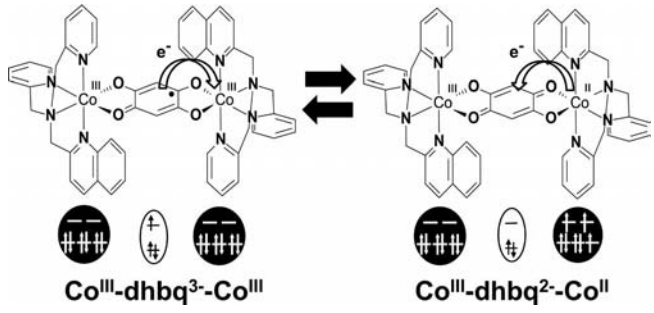

Figure 1. The molecular structure of **1** and the electronic states in the low-temperature (left) and the high-temperature (right) phases.

Results and Discussion

Electronic Spectra of 1

Figures 2 (a) and (b) show a typical diffuse reflectance electronic spectrum of the powder sample of **1** and a UV/Vis absorption spectrum of **1** in BuCN solution (3.01×10^{-5} mol/L) at room temperature, respectively. The inset in Figure 2 (b) is the expanded version of the region between 450 and 600 nm. These spectra show peaks at the wavelength λ = 538 nm in the powder sample and λ = 510 nm in the BuCN solution sample, which were assigned to the weak ligand-to-metal charge transfer (LMCT) bands from the $dhbq^{3-}$ radical to Co^{IIILS}.[17] In the investigation of LIVT, the wavelength of the laser pulse was chosen to be that of the LMCT band shown in Figure 2 (λ = 538 nm in

[a] Department of Chemistry/Material Science, Graduate School of Science, Osaka City University,
3-3-138 Sugimoto, Sumiyoshi-ku, Osaka 558-8585, Japan
E-mail: teki@sci.osaka-cu.ac.jp
[b] Institute for Material Chemistry and Engineering, Kyushu University,
Kasuga, Fukuoka 816-8580, Japan
E-mail: sato@cm.kyushu-u.ac.jp
Supporting information for this article is available on the WWW under http://dx.doi.org/10.1002/ejic.201100467.

the powder sample and λ = 510 nm in the glass sample). Although the peak positions are expected to shift slightly at low temperature, we used a broad-band optical parametrical oscillator (OPO) system (the bandwidth of the OPO pulsed laser is typically ca. 100 cm^{-1} at 600 nm) and actually covered the LMCT band inducing the LIVT transition.

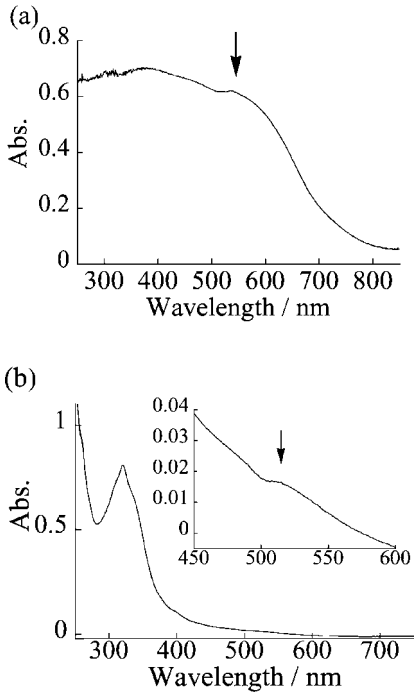

Figure 2. Absorption spectra of **1**: (a) diffuse reflectance spectrum of the powder sample, (b) UV/Vis absorption in BuCN solution. The arrows indicate the LMCT transitions.

Typical ESR Spectra of 1 and Observation of LIVT Phenomena

Figure 3 shows the typical change in the low-temperature ESR signal caused by laser light irradiation for the powder sample and for the sample diluted in a BuCN rigid glass matrix (glass sample). As shown in Figure 3, the change in the ESR signal was clearly observed in the glass sample [Figure 3 (b)] as well as in the powder sample [Figure 3 (a)], showing that valence tautomerism (VT) and LIVT phenomena occur in the glass sample. In this experiment, we used a pulsed laser (pulse width; ca. 7 ns) as the light source. The ESR signal of the $dhbq^{3-}$ ligand disappeared rapidly and almost completely as a result of irradiation with a pulsed laser at 15 K. The wavelength λ of the laser pulse was chosen to be that of the LMCT band. In the glass matrix, in the low-temperature region, the dispersion mode was mixed with the usual absorption signal because of the delay of the signal response with respect to the high-frequency (100 kHz) field modulation as a result of the long spin-lattice relaxation time. This leads to the asymmetric line shape and effectively low resolution. This problem was solved by using a low-frequency field modulation (400 Hz) in the external lock-in amplifier. Therefore, we used the low-field modulation (typically 400 Hz) in the time-profile experiments discussed later (measurement of the decay and the recovery of the ESR signal intensity).

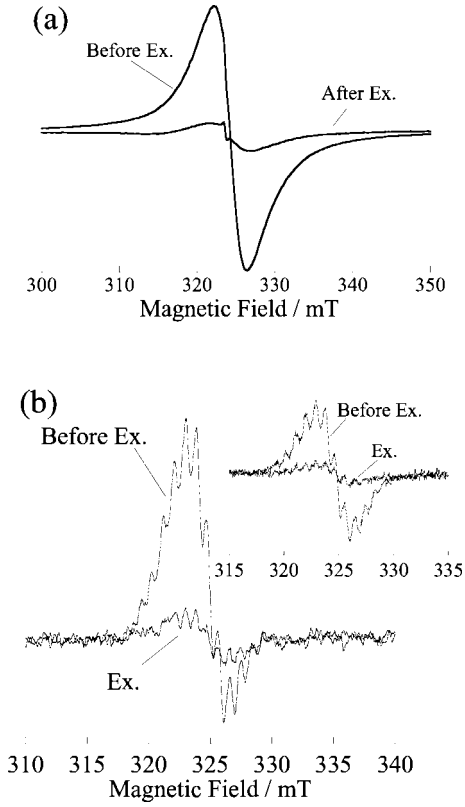

Figure 3. The change in the X-band ESR signal at 15 K as a result of laser irradiation: (a) Powder sample; excitation wavelength λ = 538 nm. (b) Diluted sample in BuCN glass matrix. The low microwave power of 0.48 μW was used and λ = 510 nm. The inset is the typical ESR spectrum observed by using the low-frequency field modulation of 400 Hz. Other spectra were measured with the 100 kHz field modulation of the conventional ESR apparatus. See also the Supporting Information.

In our previous work, approximately 25% of the material showed LIVT phenomena in the bulk sample. The present experiments show that the low efficiency of the transition observed in the previous work[12] is because of the photoirradiation (the penetration of light) with a continuous wave light source. When a pulsed laser is used as a light source, the photon density is extremely high relative to a continuous wave light source, and the light penetrates deeper into the sample. The decrease in the ESR signal intensity is due to the change of the electronic spin state from S = 1/2 ($dhbq^{3-}$) to S = 0 ($dhbq^{2-}$) by intramolecular electron transfer from the $dhbq^{3-}$ ligand to the Co^{III} metal ion (LMCT). Unfortunately, the signal of the Co ion was not clearly detected by ESR because of the unfavorably short electronic relaxation times of Co species.[18] The recovery of the signal intensity of $dhbq^{3-}$ was used as the probe of the back electron transfer due to thermal relaxation or due to the QT mechanism to be discussed later. Figure 4 shows the temperature dependence of the ESR spectra of **1** before the LIVT transition in the rigid glass matrix. As shown in the

inset of Figure 3 (b) and in Figure 4, the super-hyperfine structure (15 lines) arising from two equivalent Co nuclei (I = 7/2) was clearly detected when we used the low-frequency field modulation with the external lock-in amplifier. These spectra show that the two Co^{III} nuclei are equivalent to each other in the $Co^{III,LS}$-$dhbq^{3-}$-$Co^{III,LS}$ state.

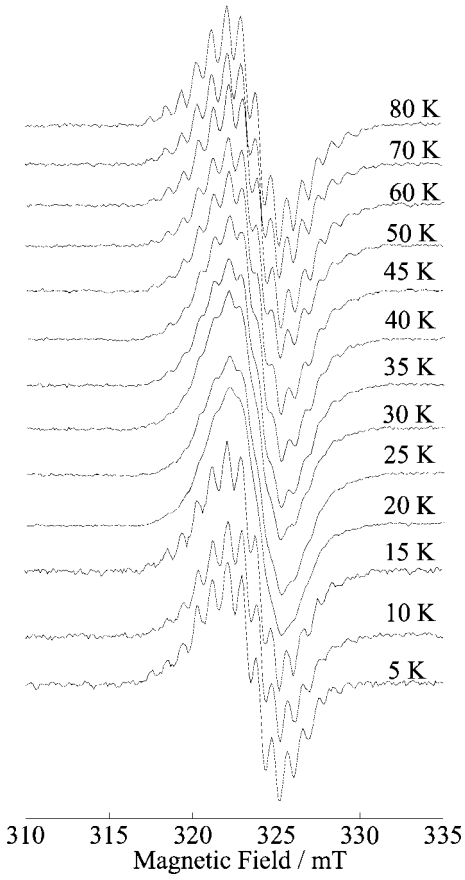

Figure 4. Temperature dependence of the ESR spectra of **1** diluted in BuCN rigid glass matrix. The low-frequency field modulation of 400 Hz was used. The super-hyperfine structure (15 lines) arising from two equivalent Co nuclei (I = 7/2) were clearly detected.

Decay and Recovery of the ESR Signal

Figure 5 shows the decay profile of the ESR signal of $dhbq^{3-}$ during light irradiation and the signal recovery after irradiation at several temperatures. The normalized signal change $[I(t) - I(t_{OFF})]/[I(0) - I(t_{OFF})]$ due to light irradiation is also shown in Figure 6, which corresponds to the ratio of molecules relaxed from the metastable phase to the low-temperature phase. Here, $I(t)$ and $I(t_{OFF})$ are the ESR signal intensities measured at time t and at the time the light was turned off, respectively. The time profiles were analyzed by double (or triple) exponential fitting as shown in Figure 8 (the detailed analysis will be discussed later). The possibility that the double exponentials arise from two nonequivalent Co sites can be ruled out, because super-hyperfine structure indicating two equivalent Co nuclei (I = 7/2) was observed, as mentioned above. In the solid, the deviations of the relax-

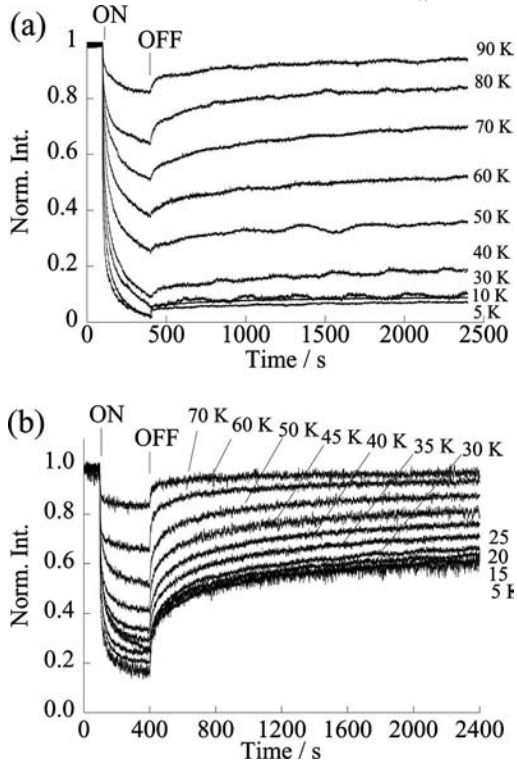

Figure 5. Temperature dependence of the ESR signal intensity of $dhbq^{3-}$ during light irradiation (ON: start of the irradiation; OFF: end of the irradiation) and the relaxation time profile after irradiation. (a) Powder sample. (b) Glass sample. The intensity was normalized to that before irradiation. In order to avoid the effect of the slow response of the ESR signal at low temperature, we used low-frequency field modulation (400 Hz) in these measurements.

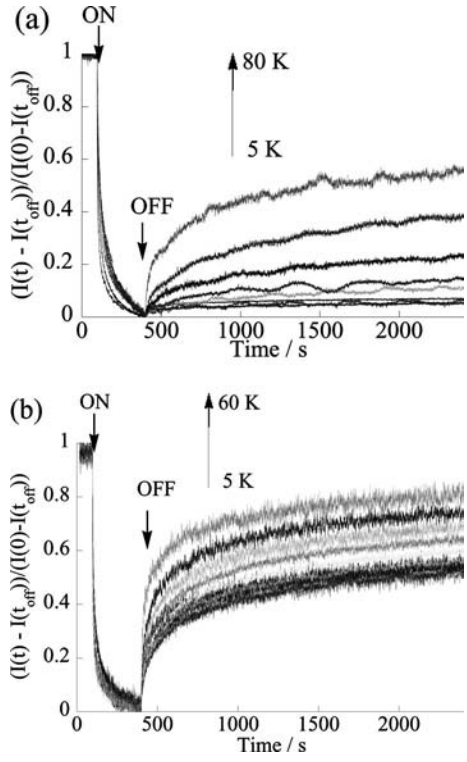

Figure 6. The normalized change in the signal $[I(t) - I(t_{OFF})]/[I(0) - I(t_{OFF})]$ after light irradiation. (a) Powder sample. (b) Glass sample.

ation curve from the single exponential are sometimes explained as intermolecular cooperative effects.[19] However, in the diluted glass matrix, the cooperative effect can be ruled out as the origin of the double exponential fitting, because such cooperative effects are not expected in the sample diluted in the glass matrix. Therefore, this finding indicates that a two-step mechanism exists.

As temperature decreases, the time profiles become independent of temperature, showing that the back electron transfer at low temperature is due to the QT mechanism, which is expected to be temperature-independent.[20] QT behavior was observed in the glass samples more clearly than it was observed in the powder sample. As shown in Figure 5 (b), the time profile did not change below 25 K in the glass sample. The temperature independence in the low-temperature region shows that the origin of the double exponential fitting is not the thermal heating of the sample by the light irradiation. With decreasing temperature, the heat capacity is decreased and the spin-lattice relaxation time is increased. Therefore, as temperature decreases, the temperature of the sample is more easily increased by light irradiation as a result of the small heat capacity, and the spin temperature goes down more slowly at low temperature as a result of the long spin-lattice relaxation time. Therefore, if the effect of thermal heating is evident, the relaxation curve profiles are expected to depend on temperature in the low-temperature region, and the temperature-independent quantum tunneling behavior is difficult to detect clearly.

Estimation of the Effective Activation Energy

In many previous works, the behaviors of the isothermal decay of the photoinduced metastable states are phenomenologically described by assuming a stretched exponential decay law. In the present case, when monitoring the ESR signal recovery, the stretched exponential law is given by Equation (1).

$$[I(t) - I(t_{OFF})]/[I(0) - I(t_{OFF})] = C\{1 - \exp[-(k_{eff}{}^{\beta}(t - t_{OFF})^{\beta})]\} \quad (1)$$

Here, β is a parameter varying from 0 to 1 and accounting for the distribution of the relaxation times. The magnitude of the estimated effective rate constants (k_{eff}) was dispersed at each temperature, although the time profiles were fitted by the above law (β = 0.6 for the powder sample and β = 0.5 for the glass matrix). Thus, it was difficult to estimate the effective activation energy of the relaxation process accurately, as shown in the Supporting Information. As an alternative way, the averaged rate constants of the relaxation were estimated from the ratios of the ESR signal recovery at approximately 2000 s after turning off the light (right ends of the curves in Figure 5). Figure 7 shows the temperature dependence of the averaged rate constants. From the linear fitting of the data of the $\log_e k_{eff}$ vs. $1/T$ curve, in the range higher than 30 K (QT is dominant below 30 K), the effective activation energies of the relaxation process in the powder and the glass samples were estimated to be 115 K (80 cm^{-1}) and 40 K (28 cm^{-1}), respectively (see the insets in Figure 7). The effective activation energy [$\Delta E(T_{eff})$] can be compared to that determined from magnetic susceptibility experiments, because the usual process of measuring the magnetic susceptibility is very slow.[21] The effective rate constant estimated by the present analysis is a kind of averaged value of the local LMCT and the whole transition. The value for the powder sample determined from the ESR experiments was smaller but had the same order of the magnitude (135 cm^{-1}) as that determined from the magnetic susceptibility measurements in our previous work.[11,22] This may be reasonable, because the activation energy estimated by the present work is not the whole activation energy from the low-temperature phase (Co^{III}-dhbq^{3-}-Co^{III} with S = 1/2) to the high-temperature phase (Co^{III}-dhbq^{2-}-Co^{II} with S = 3/2). The change in the bulk structure and in the entropy will be caused by the local LMCT. However, the activation energy may be dominated by that of the rate-determining process.

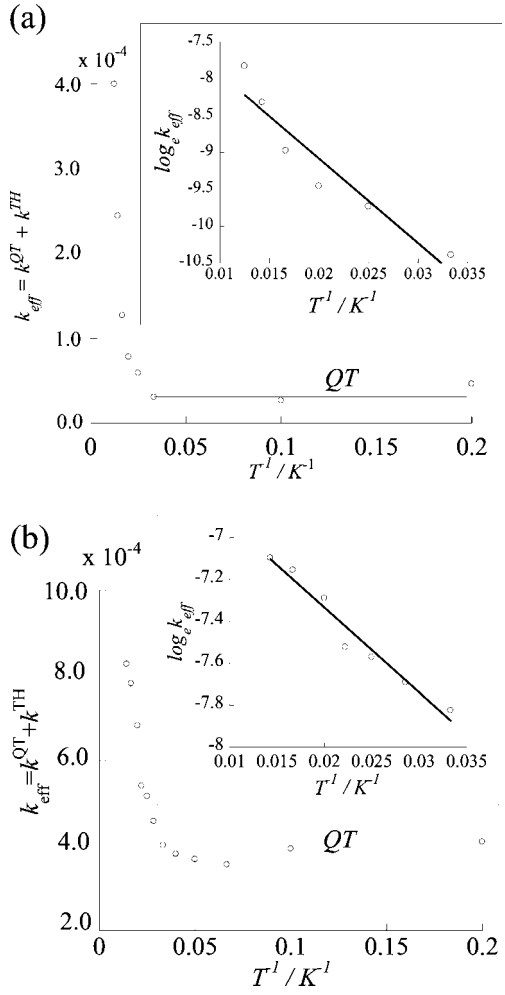

Figure 7. The temperature dependence of the averaged rate constant (k_{eff}) calculated from the normalized signal change [$I(t)$ – $I(t_{OFF})$]/[$I(0)$ – $I(t_{OFF})$] after light irradiation. The effective activation energies of the relaxation process in the powder and the glass samples were estimated from the $\log_e k_{eff}$ vs. $1/T$ plot shown in the insets. (a) Powder sample. (b) Glass sample.

Analyses of the Time Profile

Decay Process

The decay curves in Figure 5 were analyzed by using Equation (2).

$$I(t)/I(0) = 1 - \frac{k_1}{k_1 + k_2} + \frac{k_1}{k_1 + k_2} e^{-(k_1+k_2)t} + Ae^{-k_3 t} \quad (2)$$

Figure 8 (a) shows the typical examples of the analyses of the decay time profile of the glass sample during photoirradiation by the double exponential function given in Equation (2). The decay time profile fitted very well into the double exponential function. This suggests a two-step mechanism or the existence of an unknown additional relaxation mechanism. One plausible candidate for the two-step mechanism is:

$$\left[Co^{III,LS}\text{-}dhbq^{3-}\text{-}Co^{III,LS} \right] \underset{k_2}{\overset{k_1}{\rightleftharpoons}} \left[Co^{III,LS}\text{-}dhbq^{2-}\text{-}Co^{II,LS} \right] \underset{k_{3-}}{\overset{k_{3+}}{\rightleftharpoons}} \left[Co^{III,LS}\text{-}dhbq^{2-}\text{-}Co^{II,HS} \right]$$

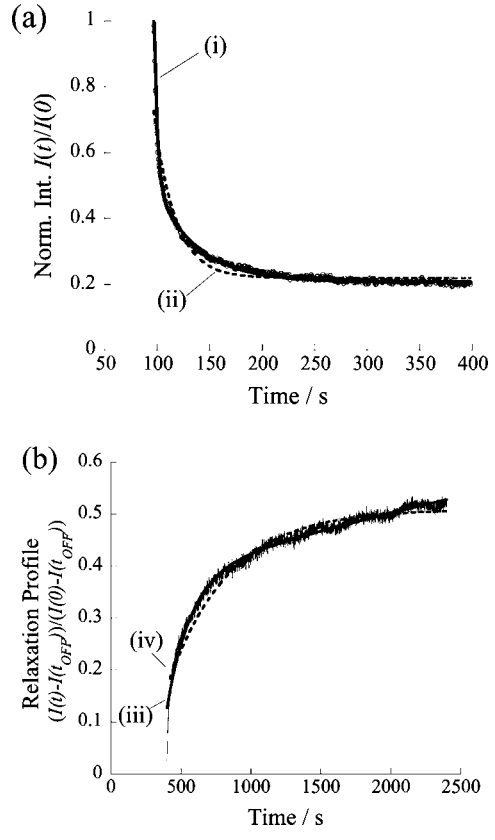

Figure 8. Analysis of the decay and the relaxation profiles. (a) Decay profile of the glass sample during light irradiation at 20 K; (i) and (ii) are double and single exponential fittings, respectively. (b) Relaxation of the normalized signal change in the glass sample at 20 K after light irradiation; (iii) and (iv) are double and single exponential fittings, respectively.

Here, k_1, k_2, and k_3 are the rate constants of each step. The last term in Equation (2) is the effective relaxation term described by k_{3+} and k_{3-}, which is related with the structure and entropy changes between the LS and the HS state. The typical values of the rate constants in the decay process of the glass sample were $k_1 = 2.6 \times 10^{-1}$ s^{-1}, $k_2 = 7.0 \times 10^{-2}$ s^{-1}, and $k_3 = 2.5 \times 10^{-2}$ s^{-1} at 20 K, as shown in Figure 8. Unfortunately, we could not detect directly the ESR signal of the metastable photoinduced product $Co^{III,LS}$-$dhbq^{2-}$-$Co^{II,LS}$ because of its short lifetime and the unfavorably short electronic relaxation time of the $Co^{II,LS}$ species.[18] However, if the LIVT of **1** is a single-step process and there is no additional (unknown) relaxation mechanism (no cooperative effects being expected in the glass matrix), the last term in Equation (2) can be omitted, and the decay curves can be analyzed by single exponential fitting.

The temperature dependence of the term $k_1/(k_1 + k_2)$ in the decay process of Equation (2) is given in Figure 9. The values were obtained by least-squares fitting of the decay profiles at each temperature. In addition, we also carried out the analyses for the hypothesis of the two-step mechanism. There are expected to be two temperature-independent mechanisms of the ESR signal decay of $dhbq^{3-}$. One is the LMCT induced by the light irradiation (k_{LMCT}) and the other is the temperature-independent QT effect (k_{QT1}). The rate constants due to the thermal activation processes in the ESR signal decay were neglected here, because the rate of the LMCT is much faster than that of the thermal activation process at low temperature. The rate constant of QT in the relaxation (ESR signal recovery) is k_{QT2}. The thermal relaxation processes (back electron transfer) are expressed by $k_{TR}\exp(-E_{BET}/k_BT)$, where E_{BET} denotes the activation energy for the back electron transfer. Therefore, the rate constants of the signal decay (k_1) and the signal recovery (k_2) are given by $k_1 \approx k_{LMCT} + k_{QT1}$ and $k_2 = k_{QT2} + k_{TR}\exp(-E_{BET}/k_BT)$, respectively. The term $k_1/(k_1 + k_2)$ is given by Equation (3).

$$\frac{k_1}{k_1 + k_2} = \frac{k_{LMCT} + k_{QT1}}{k_{LMCT} + k_{QT1} + k_{QT2} + k_{TR}\exp(-E_{BET}/k_BT)} \quad (3)$$

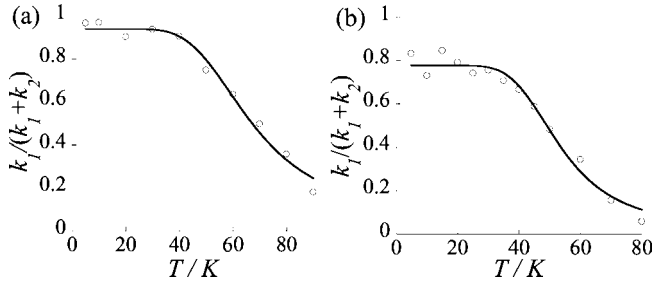

Figure 9. Temperature dependence of the term $k_1/(k_1 + k_2)$ in Equation (2) determined by the decay process during light irradiation. (a) Powder sample. (b) Glass sample.

The temperature dependences of the term $k_1/(k_1 + k_2)$ in the powder and glass samples were fitted by using Equation (3) as shown in Figure 9. In these fittings, it is not nec-

essary to introduce the β factor as in the stretched exponential law. We can only estimate the ratios $k_{QT2}/(k_{LMCT} + k_{QT2})$ and $k_{TR}/(k_{LMCT} + k_{QT2})$ and the energy barrier of the LMCT state. The least-squares fitting gave E_{BET} = 308 K for the powder sample and E_{BET} = 299 K for the glass sample, respectively. It should be noted that these values are the thermal activation energies of the back electron transfer of the first step within the two-step mechanism during the photoexcitation, which is related to the potential barrier of the back electron transfer. These values were of the same order of the magnitude but larger than the effective activation energies of the relaxation process in the powder and glass samples, which were estimated to be 115 K (80 cm^{-1}) and 40 K (28 cm^{-1}), respectively, from the normalized signal change after light irradiation. If the second step is the rate-determining process, the effective activation energy is close to the energy difference between the low-temperature phase (Co^{III}-$dhbq^{3-}$-Co^{III} with S = 1/2) and the high-temperature phase (Co^{III}-$dhbq^{2-}$-Co^{II} with S = 3/2). Therefore, E_{BET} and the effective activation energy do not need to be related. The estimated E_{BET} vales are close to each other in the powder sample and the glass sample. However, as shown in Figure 5, the rate of QT in the glass sample is apparently much faster than that in the powder sample (QT phenomena are clearly observed in the glass sample). If the estimation is accurate enough (in the present approximation, the effect of thermal activation on the ESR signal decay was neglected), this finding indicates that the potential barrier of the second step in the glass sample is lower than that in the powder sample.[23]

Relaxation Process

As shown in Figure 8 (b), the relaxation of the normalized signal change $[I(t) - I(t_{OFF})]/[I(0) - I(t_{OFF})]$ was also fitted to the double exponential relation given in Equation (4).[24]

$$(I(t)-I(t_{OFF}))/(I(0)-I(t_{OFF}))=1-Be^{-k_4t}-Ce^{-k_5t} \quad (4)$$

This finding also indicates the possibility of a two-step mechanism, as discussed above. The typical values of the rate constants in the relaxation process of the glass sample are $k_4 = 5.9 \times 10^{-3}\ s^{-1}$ and $k_5 = 1.3 \times 10^{-4}\ s^{-1}$ at 20 K, as shown in Figure 8. The rate constants of the relaxation process are slower by one order of magnitude than those of the process induced by laser irradiation. Recently, it was reported that the relaxation mechanism between the HS state of Co^{II} and the LS state of Co^{III}, which is observed in a similar valence tautomeric compound, $[Co(sq)_2(bpy)]$ (sq = semiquinone; bpy = 2,2′-bipyridine), was expected to be a one-step mechanism, according to the energy of the three spin states and the crossing points obtained by the ab initio molecular orbital calculations with the DFT method.[25] In our results that support a two-step mechanism, the electrons transferred from the dhbq ligand go to the next state, which is the transient LS state of Co^{II}. Since this transient state is a low-lying state with a short lifetime, it may be out of the scope of the accuracy of the ab initio DFT calculation reported previously. Our results support the possibility of the two-step mechanism proposed in the literature.[26] In this paper it was discussed as a possibility that spin crossover from $Co^{II,HS}$ to $Co^{II,LS}$ occurs upon decreasing the temperature, and a further decrease leads to intramolecular electron transfer from $Co^{II,LS}$ to $Co^{III,LS}$. Our LIVT phenomenon is the reverse of the process induced by light irradiation, because we start from the $Co^{III,LS}$ state and reach the $Co^{II,HS}$ state. Therefore, the present results indicate the above two-step mechanism. The relaxation rate in the glass sample is evidently faster than that in the powder sample, as clearly shown in Figure 5. Thus, the effective thermal activation energy of the glass sample is smaller than that of the powder sample. The rate constant of the QT mechanism in the glass matrix is also greater than that in the powder samples. This means that a change in structure is more difficult in the solid (powder sample) relative to that in the glass sample, because the molecular structure is more rigidly fixed by the neighboring molecules in the solid. In this paper, we can analyze the observed experimental data by assuming a two-step mechanism. However, it is noted that the two-step mechanism is the most plausible hypothesis at the moment, because the direct observation of the signal of the $Co^{II,LS}$ ion was not possible by ESR analysis because of the unfavorably short electronic relaxation time of Co species. To confirm these findings, a similar study is planned on the mononuclear Co LIVT complex.

Conclusions

LIVT of dinuclear Co complex **1** was investigated by low-temperature ESR analysis in a glass matrix as well as in a powder sample. Almost complete VT was detected by using pulsed laser irradiation. QT was clearly observed in the glass matrix at low temperature. From the analyses of the time profiles of the decay and the relaxation, the possibility of a two-step mechanism was suggested, in which the first step is the local electron transfer (LMCT) from the $dhbq^{3-}$ ligand to the LS Co^{III} ion and the second step is the spin state transition from LS Co^{II} to HS Co^{II}, due to the geometrical change from a strong crystal field to a weak one. The effective activation energy was estimated by using the ESR signal of $dhbq^{3-}$ as the probe.

Experimental Section

Materials and Sampling Procedure: Dinuclear Co complex **1** was synthesized as described in our previous report.[12] In the measurements on the diluted glass sample, we used butyronitrile (BuCN) as the glass matrix. GR grade BuCN was purchased from Tokyo Kasei Kogyo Co. Ltd. It was dehydrated with CaH_2 for one week and was further purified by distillation.

ESR Measurements: Conventional continuous wave ESR spectra were measured by a commercially available continuous wave ESR spectrometer (JEOL TE300) with a cooled He gas flow cryostat (Oxford ESR910). For the time-profile experiments, the ESR signal

detected by the diode was pre-amplified with a microwave transmission circuit and transferred to an external lock-in amplifier (EG&G Model 5210). The detected signal was transferred to a personal computer that was part of the of the ESR system by using a general purpose interface bus (GPIB). For the ESR experiments with low-frequency field modulation, external filed modulation was available in our system up to 1 kHz. The experiments were carried out by using the external field modulation coil attached to the magnet of the ESR system. The system was controlled by a home-made control program written by using LABVIEW (National Instrument). In the glass matrix, we used very low microwave power in the low-temperature experiments in order to avoid power saturation (typically 40 μW at 30 K and 0.48 μW at 15 K). A Nd:YAG pulsed laser (Continuum Surelite II) connected to an OPO system (Continuum Surelite OPO) was used as the light source. The typical output laser power was approximately 4–5 mJ (the laser beam was spread to a diameter of approximately 1 cm^2 at the sample position). The temperature was controlled by a temperature control system (Oxford ITC503). In the ESR experiment, the glass samples were degassed by repeated freeze-pump-thaw cycles. All ESR experiments were carried out in the low-temperature phase (LS phase).

Electronic Spectra Measurements: UV/Vis absorption spectra and diffuse reflectance spectra were measured at room temperature with a HITACHI U-3500 T UV/Vis/NIR spectrometer without and with an integrating sphere, respectively.

Supporting Information (see footnote on the first page of this article): Change in the X-band ESR signal as a result of laser irradiation in the glass matrix and additional analysis of the relaxation profile.

Acknowledgments

Y. T. is grateful to the Japan Society for the Promotion of Science (JSPS), Japan for a Grant-in-Aid for Scientific Research on General Research (B) (No. 21350081).

[1] C. G. Pierpont, *Coord. Chem. Rev.* **2001**, *99*, 216–217.
[2] P. Gütlich, A. Dei, *Angew. Chem.* **1997**, *109*, 2852; *Angew. Chem. Int. Ed. Engl.* **1997**, *36*, 2734–2736.
[3] D. A. Shultz in *Magnetism: Molecules to Materials II* (Eds.: J. S. Miller and M. Drillon), Wiley-VCH, Weinheim, **2001**, p. 281.
[4] E. Evangelio, D. Ruiz-Molina, *Eur. J. Inorg. Chem.* **2005**, 2957–2971.
[5] O. Sato, J. Tao, Y.-Z. Zhang, *Angew. Chem.* **2007**, *119*, 2200; *Angew. Chem. Int. Ed.* **2007**, *46*, 2152–2187.
[6] P. Gütlich, A. Hauser, H. Spiering, *Angew. Chem.* **1994**, *106*, 2109; *Angew. Chem. Int. Ed. Engl.* **1994**, *33*, 2024–2054.
[7] A. Dei, D. Gatteschi, C. Sangregorio, L. Sorace, *Acc. Chem. Res.* **2004**, *37*, 827–835.
[8] R. D. Schmidt, D. A. Shultz, J. D. Martin, P. D. Boyle, *J. Am. Chem. Soc.* **2010**, *132*, 6261–6273.
[9] Y. Mulyana, G. Poneti, B. Moubaraki, K. S. Murray, B. F. Abrahams, L. Sorace, C. Boskovic, *Dalton Trans.* **2010**, *39*, 4757–4763.
[10] J. Tao, H. Maruyama, O. Sato, *J. Am. Chem. Soc.* **2006**, *128*, 1790–1791.
[11] O. Sato, T. Iyoda, A. Fujishima, K. Hashimoto, *Science* **1996**, *272*, 704–705.
[12] B. Li, J. Tao, H.-L. Sun, O. Sato, R.-B. Huang, L.-S. Zheng, *Chem. Commun.* **2008**, 2269–2271.
[13] C. Carbonera, A. Dei, J.-F. Létard, C. Sangregorio, L. Sorace, *Angew. Chem.* **2004**, *116*, 3198; *Angew. Chem. Int. Ed.* **2004**, *43*, 3136–3138.
[14] A. Beni, A. Dei, D. A. Shultz, L. Sorace, *Chem. Phys. Lett.* **2006**, *428*, 400–404.
[15] D. M. Adams, D. N. Hendrickson, *J. Am. Chem. Soc.* **1996**, *118*, 11515–11528.
[16] A. Dei, G. Poneti, L. Sorace, *Inorg. Chem.* **2010**, *49*, 3271–3277.
[17] The corresponding LMCT bands were reported to appear at 492 and 536 nm at room temperature in the diffuse reflectance spectrum of the compound similar to **1** in ref.[10] These bands were observed at 500–600 nm at 80 K and at approximately 620 nm in the other similar compound reported in ref.[13]
[18] L. Banci, A. Bencini, C. Benelli, D. Gatteschi, C. Zanchini, *Struct. Bonding (Berlin)* **1982**, *52*, 37–86.
[19] J.-F. Létard, P. Guionneau, L. Rabardel, J. A. K. Howard, A. E. Goeta, D. Chasseau, O. Kahn, *Inorg. Chem.* **1998**, *37*, 4432–4441.
[20] The existence of QT in the low-temperature region was also indicated by the measurement of magnetic susceptibility of the powder sample.[12] However, in the glass sample, this mechanism was clearly demonstrated by the dominant relaxation mechanism below 30 K.
[21] The expected maximum deviation between the present analyses (ΔE_{eff}) and the value ($\Delta E_{stretched\ fit}$) obtained by the stretched exponential fitting is $\Delta E_{eff} = \beta \Delta E_{stretched\ fit}$. The values obtained by the present analyses will therefore be slightly lower, because $\beta < 1$.
[22] By using $\beta = 0.6$ obtained by the stretched exponential fit for ESR signal recovery in the powder sample, $\Delta E_{stretched\ fit}$ can be estimated to be 133 cm^{-1}, which is close to the magnitude determined from the susceptibility measurements.
[23] According to the WKB (Wentzel–Kramers–Brillouin) approximation, the transmission coefficient P of quantum tunneling is given by

$$P = \exp[-(2/\hbar)\int_{r1}^{r2} \sqrt{2m(V(r) - E)}dr]$$

Here, $V(r)$ and E are the potential and the energy of the state, respectively. Therefore, P depends on the height of the potential barrier, $V(r) - E$.
[24] In the relaxation process, an additional rapid component of the same order of magnitude as that of k_2 in Equation (2) may exist as shown in Figure S2 in the Supporting Information.
[25] D. Sato, Y. Shiota, G. Juhász, K. Yoshizawa, *J. Phys. Chem. A* **2010**, *114*, 12928–12935.
[26] C. Roux, D. M. Adams, J. P. Itié, A. Polian, D. H. Hendrickson, M. Verdaguer, *Inorg. Chem.* **1996**, *35*, 2846–2850.

Received: May 3, 2011
Published Online: August 2, 2011

